J Neuropathol Exp Neurol

Vol. 68, No. 8
August 2009
pp. 845–856

ORIGINAL ARTICLE

Enhanced Microglial Clearance of Myelin Debris in T Cell-Infiltrated Central Nervous System

Helle Hvilsted Nielsen, MD, Rune Ladeby, MD, PhD, Christina Fenger, MSci, Henrik Toft-Hansen, PhD, Alicia A. Babcock, PhD, Trevor Owens, PhD, and Bente Finsen, MD, DMSc

Abstract

Acute multiple sclerosis lesions are characterized by accumulation of T cells and macrophages, destruction of myelin and oligodendrocytes, and axonal damage. There is, however, limited information on neuroimmune interactions distal to sites of axonal damage in the T cell-infiltrated central nervous system. We investigated T-cell infiltration, myelin clearance, microglial activation, and phagocytic activity distal to sites of axonal transection through analysis of the perforant pathway deafferented dentate gyrus in SJL mice that had received T cells specific for myelin basic protein (T_{MBP}) or ovalbumin (T_{OVA}). The axonal lesion of T_{MBP}-recipient mice resulted in lesion-specific recruitment of large numbers of T cells in contrast to very limited T-cell infiltration in T_{OVA}-recipient and -naïve perforant pathway-deafferented mice. By double immunofluorescence and confocal microscopy, infiltration with T_{MBP} but not T_{OVA} enhanced the microglial response to axonal transection and microglial phagocytosis of myelin debris associated with the degenerating axons. Because myelin antigen-specific immune responses may provoke protective immunity, increased phagocytosis of myelin debris might enhance regeneration after a neural antigen-specific T cell-mediated immune response in multiple sclerosis.

Key Words: Dentate gyrus, Microglia, Myelin basic protein, Perforant pathway, Phagocytosis, T cells.

INTRODUCTION

T cells reactive to myelin proteins are considered to have crucial pathogenetic roles in inflammatory responses in multiple sclerosis (MS) (1, 2); they accumulate in the cerebrospinal fluid and in MS lesions (3, 4). Pathogenetic roles for myelin antigen-specific T cells are supported by studies on the animal model experimental autoimmune encephalomyelitis (EAE), in which clinical and histologic features similar to those in MS can be induced in naïve recipients by adoptive transfer of myelin antigen-reactive T cells (5–7). There is, however, also evidence that the injured central nervous system (CNS) can benefit from T-cell responses to myelin antigens. For example, T cells reactive to myelin basic protein (MBP) but not to ovalbumin protect neurons from secondary degeneration in different CNS injury models (8–10). This protective autoimmunity involves various mechanisms that include secretion of the anti-inflammatory cytokine interleukin (IL) 10 (10) or the neurotrophic factors neurotrophic factor 3 and brain-derived neurotrophic factor (11, 12), and the induction of "functional silencing" in damaged neurons (8, 13).

Microglial responses in CNS injury and disease can also be harmful or beneficial, depending on the stimulus they receive (14, 15). Microglia are the principal phagocytic cell in the CNS (16, 17), which, when activated, produce cytokines, neurotrophins, and immunomodulatory factors. Although microglia are ubiquitous in the CNS, myelin debris may persist for several months after injury in the absence of inflammation (18–20). Because myelin debris inhibits remyelination and neurite outgrowth (21, 22), this raises the possibility that inflammation might stimulate microglial phagocytosis of myelin debris, which would then disinhibit regenerative processes and remyelination (23, 24). Indeed, there is a correlation between activated phagocytic microglia and clinical recovery in optic nerve injury (25), in which there is significant T-cell infiltration (8, 26, 27). Compared with optic nerve injury (8, 26, 27) and spinal cord injury (28), T-cell infiltration into the CNS is more limited when there is minimal breakdown of the blood–brain barrier, such as from a lesion of the perforant pathway (PP) (29–32). The PP is a myelinated nerve tract that arises in the entorhinal cortex and terminates in the outer part of the molecular layer (oml) of the dentate gyrus (33, 34). Transection of the PP results in anterograde axonal and a dense terminal degeneration in the oml of the dentate gyrus (35), causing accumulation of myelin debris that persists for several weeks until it is eventually cleared by phagocytic microglia (36–39).

To investigate the effect of myelin-reactive T cells on the microglial response to axonal degeneration and microglial

From the Medical Biotechnology Center, University of Southern Denmark, Winsløwparken 25, DK-5000 Odense C, Denmark.
Send correspondence and reprint requests to: Helle Hvilsted Nielsen, Medical Biotechnology Center, University of Southern Denmark, Winsløwparken 25, Second Floor, DK-5000 Odense C, Denmark; E-mail: hhnielsen@health.sdu.dk
Supported by the Danish Multiple Sclerosis Society, Michaelsen Foundation, the Graduate School of Immunology, the Danish Medical Association's Research Foundation, Director Leo Nielsen's Foundation, Bent Bøgh and Wife's Foundation, the Foundation for Promotion of Medical Research, Frimodt-Heineke Foundation, King Christian X's Foundation, Merchant Brogaard's Foundation, the Senior Hospital Physician's Foundation, Karen A. Tholstrup's Foundation, Chief Physician Dr. Med. Alfred Helsted's Grant, Foundation for Neurological Research, Dir. Frimodt's Foundation, Hede Nielsen's Foundation, Kurt Bønnelycke's Foundation, Torben og Alice Nielsen's Foundation, Fru Lily Benthine Lund's Foundation, Dir. Jacob Madsen and Wife Olga Madsen's Foundation, Beckett-Foundation and Warwara Larsen's Foundation, and European Cooperation in the field of Scientific and Technical Research Organization.

clearance of degenerated myelin, we adoptively transferred MBP-specific T cells (T_{MBP}) or ovalbumin-specific T cells (T_{OVA}) into recipient mice and induced a PP lesion. We found that an axonal lesion in T_{MBP}-recipient mice not in T_{OVA}-recipient mice resulted in extensive T-cell infiltration in the deafferented oml of the dentate gyrus and that there was enhanced clearance of myelin debris due to increased phagocytosis by activated microglia. These results raise the possibilities that axonal degeneration might precipitate the development of new inflammatory lesions and that infiltration of myelin-reactive T cells could be beneficial to the regenerative process by increasing phagocytosis of degenerating myelin.

MATERIALS AND METHODS

Animals, Manipulation of Animals, and Tissue Processing

Animals

Female SJL mice (8–10 weeks) were obtained from Bomholtgaard (Skensved, Denmark) and the Jackson Laboratory (Bar Harbor, ME). Mice were kept in a pathogen-free, temperature and humidity-controlled environment with 12-hour light-dark cycle and provided with food and water ad libitum. Experiments were approved by the National Danish Animal Care Committee (Permission no. 192000/561-272 and J.nr. 192000/51-272).

Transfer of T Cells

$CD4^+$ T_{MBP} and T_{OVA} were generated as previously described (40, 41) and injected intravenously to recipient mice (n = 19 and n = 12, respectively). Donor mice were immunized 7 days apart by 2 subcutaneous injections at the base of the tail and in the flank with 50 μL of an emulsion made of complete Freund adjuvant containing 0.5 mg/mL of *Mycobacterium tuberculosis* (ICN Biomedicals, Inc., Aurora, OH) and MBP (Sigma, St. Louis, MO; 4 mg/mL) or Ovalbumin (Fluka; 60 mg/mL). Lymph nodes were collected on day 14, and cells were cultured for 4 days in RPMI-1640 media (catalog no. 31870-017; Gibco) containing 10% fetal bovine serum (FBS; cat. no. 10500-056; Gibco), 2 mmol/L of L-glutamine (Sigma), 50 μmol/L of 2-mercaptoethanol (Bie & Berntsen, Rødovre, Denmark), and 50 μg/mL of MBP. Cells were collected on a Ficoll-Hypaque gradient (Amersham Pharmacia, Uppsala, Sweden), counted, and injected intravenously to recipient mice (5×10^6 blasts/mouse, corresponding to 28%–30% of the cells injected). T_{MBP}- and T_{OVA}-recipient mice (hereafter referred to as T_{MBP} and T_{OVA} mice, respectively) were weighed and clinically evaluated each day for the development of neurologic signs. The T_{MBP} and T_{OVA} mice showed no neurologic signs before or after lesion of the PP; unlesioned T_{MBP} mice were allowed to develop clinical EAE to increase the possibility of T-cell infiltration into the hippocampus.

PP Transection

Anterograde axonal degeneration was induced by stereotactic transection of the entorhino-hippocampal PP using a wire-knife, as described previously (42). To determine whether PP lesion induces infiltration of myelin-reactive T cells, 14 T_{MBP} and 8 T_{OVA} mice were subjected to a PP lesion 4 days after T-cell transfer, at which time myelin-reactive T cells usually enter the CNS after intravenous injection (43). The mice were killed 7 days after lesion (11 days after T-cell transfer), along with a group of naïve mice that had only been subjected to a PP lesion (n = 12); this was sufficient time for the Wallerian degeneration to give rise to MBP^+ particles and marked reactive microgliosis (37). The T_{OVA} mice were killed 11 days after T cells, and the T_{MBP} mice were killed 11 to 14 days after T-cell transfer, with signs of EAE grade 2 to 3. Unoperated SJL mice (n = 6) and unlesioned contralateral dentate gyrus served as controls.

Fixation and Tissue Sectioning

Mice were deeply anesthetized with 0.05 mL pentobarbital (200 mg/mL) and perfused through the left ventricle using 5 mL of chilled 0.15 mol/L Sørensen phosphate buffer (pH 7.4), followed by 20 mL of chilled 4% paraformaldehyde in 0.15 mol/L Sørensen phosphate buffer (pH 7.4). The brains were postfixed in 4% paraformaldehyde for 1.5 hours, immersed in 20% sucrose overnight, frozen using CO_2-snow, and stored at −20°C until they were serially cut into 16-μm cryostat sections. Some sections were stained with toluidine blue for visualization of general histopathologic changes. Remaining sections were stored at −40°C until immunohistochemical staining.

Immunohistochemistry

Standard Protocols

For validation of the quality of lesion and evaluation of microglial responses, monoclonal rat anti-Mac-1/CD11b antibody (MCA711; Serotec, Oslo, Norway; dilution, 1:600) (37, 44) was used with biotinylated species-specific monoclonal goat anti-rat antibody (RPN 1005; Amersham, Buckinghamshire, UK; dilution, 1:200) and streptavidin-horseradish peroxidase (DAKO A/S, Glostrup, Denmark; dilution, 1:200). Sections were thawed and dried for 30 minutes at room temperature (RT), followed by rinsing 3 × 15 minutes in 0.05 mol/L Trizma base–phosphate-buffered saline (TBS) containing 1% Triton (T-TBS; Sigma). After blocking of nonspecific staining with TBS containing 10% FBS, sections were incubated overnight with primary antibody diluted in 10% FBS at 4°C. Sections were then rinsed 3 × 15 minute in T-TBS and incubated with the secondary biotinylated antibodies for 1 hour at RT. Endogenous peroxidase activity was then blocked with H_2O_2 and methanol in a 1:500 mixture for 30 minutes, followed by rinsing in T-TBS for 3 × 15 minutes. Finally, sections were incubated with streptavidin-horseradish peroxidase for 1 hour at RT, rinsed in TBS 3 × 15 minutes, and developed with 0.5 mg/mL of diaminobenzidine (Sigma) in TBS for 5 to 10 minutes. After a quick rinse in TBS, sections were dehydrated through graded alcohol solutions, cleared in xylene, and mounted with DePeX (BDH Laboratory Supplies, Poole, UK).

For visualization of T cells and T-cell subsets, sections were incubated with rat anti-human CD3 (Serotec; dilution, 1:200) and rat anti-mouse CD4 and CD8 antibodies (Pharmingen, BD Biosciences; dilutions, 1:600 and 1:100, respectively). The staining procedure was as outlined for Mac-1, using histochemical detection with diaminobenzidine. Cross-reactivity of the anti-human CD3 antibody for murine CD3 was confirmed by location of $CD3^+$ cells to the periarteriolar sheath in murine spleen sections. Myelin and myelin debris were visualized using primary polyclonal rabbit anti-human MBP antibody (A0623; DAKO; dilution, 1:500), followed by incubation with alkaline phosphatase-conjugated anti-rabbit immunoglobulin (Ig) antibody (A3812, Sigma; dilution, 1:100) and development using 5-bromo-4-chloro-3-indolyl phosphate and nitro blue tetrazolium as chromogens according to Fenger et al (38).

Double Immunofluorescence

For simultaneous visualization of the endothelial basal lamina and the glia limitans, a rabbit anti-mouse laminin 1 (Cedarlane Laboratories; dilution, 1:80) was used, followed by an Alexa 594-conjugated secondary antibody goat antirabbit (A-11012; Invitrogen; dilution, 1:500). $Mac\text{-}1^+$ microglia and macrophages were detected by Alexa 488-conjugated Streptavidin (S-32354; Invitrogen; dilution, 1:500), as were $CD3^+$ T cells. For visualization of phagocytosis by activated microglia, we performed double labeling with MBP that was detected by Alexa 594-conjugated goat antirabbit (A-11012; Invitrogen; dilution, 1:500). Degenerating myelinated axons were visualized using fluorescent double labeling for neurofilament (NF; rat antimouse; Chemicon; dilution, 1:100) and MBP and detected by Alexa 488-conjugated SA together with Alexa 594-conjugated goat antirabbit. The cellular nuclei were visualized using the nucleic acid stain 4′,6-diamino-2-phenylindole (DAPI; Invitrogen; D3571), which was added in a concentration of 300 nmol/L to the TBS during the last rinse.

Controls

Nonspecific staining was assessed by incubation without the primary antibody, with an isotype-specific control (rat IgG1 or rat IgG2; Nordic Biosite AB, Täby, Norway), or with rabbit serum (X0902; DAKO), and there was no staining.

Quantitative Analysis

Cell Counting

The total number of $CD3^+$, $CD4^+$, and $CD8^+$ cells in the temporal dentate gyrus were counted in PP-lesioned T_{MBP} mice (n = 14) and compared with PP-lesioned T_{OVA} mice (n = 8), PP-lesioned naïve animals (n = 12), and unlesioned T_{MBP} (n = 5), T_{OVA} (n = 4), and naïve (n = 6) mice. Cells were counted in 5 parallel sections, each 160-μm apart in the ipsilateral deafferented and contralateral unlesioned molecular layer. In naïve mice, both hippocampi were analyzed, and the results for this group were averaged. Cell counting was performed using a 20× objective (total magnification, 200×) mounted on an Olympus 51 microscope, stepping through and counting all $CD3^+$, $CD4^+$, or $CD8^+$ cells in the molecular layer.

The numbers of $Mac\text{-}1^+$ cells in the molecular layer were counted in sections parallel to those used for T-cell counting. Cells were counted in a fixed fraction (37.5%) of the molecular layer in 5 sections, separated by 160 μm containing the temporal part of the hippocampus using the computer-assisted stereologic test GRID system (Olympus, Silkeborg, Denmark). Cells were counted using a 100× objective (total magnification, 1,000×). The total numbers (n) of $Mac\text{-}1^+$ cells contained within 5 parallel sections were estimated using the formula Estimate of $n = Q \times 1 / asf$ (area sampling fraction; 3,753/10,000) (45).

Intraparenchymal Location of Infiltrating T Cells and Macrophages

To evaluate the infiltration of T cells and macrophages in the neuropil, we selected 3 animals with high numbers of infiltrating cells. Parallel sections (n = 5) from each animal were subjected to double immunofluorescence staining for laminin 1 and CD3 or Mac-1, respectively. Sections were assessed for perivascular or intraparenchymal location of the cells.

Scoring of Myelin Deposits

To determine whether myelin disintegration and clearance of myelin debris in deafferented dentate gyrus were affected by infiltrating T_{MBP}, the amount of MBP^+ particles in the oml of the dentate gyrus of PP-lesioned T_{MBP} mice was scored and compared with PP-lesioned T_{OVA} and naïve mice and unlesioned T_{MBP}, T_{OVA}, and naïve mice. The animals were scored in a blinded fashion using a 10× objective by 2 independent observers using a range from 0 to 3 as follows: 0 for no myelin deposits, 1 for sporadic myelin deposits, 2 for moderate myelin deposits, and 3 for abundant myelin deposits (37).

Counting of Myelin Phagocytosing Microglia

For this analysis, we selected the animals with the most T cells in the oml. Sections were first analyzed using an Olympus BX51 microscope using FITCH (excitation spectrum [ex.], 460–490 nm; emission spectrum [em.], 580–750 nm), TRICH (ex., 460–490 nm; em., 510–550 nm), and DAPI (ex., 330–385 nm; em., 420–600 nm) filters. $Mac\text{-}1^+$ cells were defined by having a blue $DAPI^+$ nucleus surrounded by green $Mac\text{-}1^+$ plasmalemma. Myelin basic protein containing $Mac\text{-}1^+$ cells in addition had red MBP^+ particles within their cytoplasm, yielding a yellow color. Pictures were obtained using a 60× lens and an Olympus DP70 camera. Double- and single-labeled cells in individual mice were counted based on images obtained from the oml.

The intracellular location of the phagocytosed MBP^+ particles was validated using confocal laser scanning fluorescence microscopy (Olympus FV1000) using a 20× (numerical aperture, 0.95) Olympus water immersion objective. For the confocal analysis, the scanning area was set to 1,024 × 1,024 pixels with and without internal zoom. DAPI (Invitrogen; D3571), Alexa Fluor 488 (Invitrogen; S-32354),

and Alexa Fluor 594 (Invitrogen; A-11012) were excited sequentially with lasers at 405-, 488-, and 594-nm wavelengths. Fluorescence was monitored through 425- to 475-, 500- to 545-, and 575- and 675-nm band-pass filters (acousto-optical tunable filter), respectively.

Statistics

Group values are given as medians. Group medians for ipsilateral and contralateral data were compared using 1-tailed paired Student *t* test. For the remaining data group, medians were compared using the Kruskal-Wallis test, followed by 2-sample Wilcoxon rank sum (Mann-Whitney) test or by Mann-Whitney test. All tests were made using STATA (StataCorp LP, College Station, TX). p values are indicated as follows: *, $p < 0.05$; **, $p < 0.01$; and ***, $p < 0.001$.

RESULTS

Validation of Lesion of T Cell-Recipient and -Naïve Mice

Transection of the PP resulted in reactive microgliosis in the deafferented zone, as previously described (37, 46–48). Mice with a complete PP lesion had a clearly demarcated band of reactive Mac-1$^+$ microglia restricted to the deafferented oml of the dentate gyrus. Mice that did not display a band of reactive microglia were excluded from the study, as were animals in which the lesion encroached on the dentate gyrus.

Targeting of T Cells to the Zone of Axonal Degeneration

PP lesion of T_{MBP} mice induced a massive infiltration of CD3$^+$ T cells, especially in the oml of the dentate

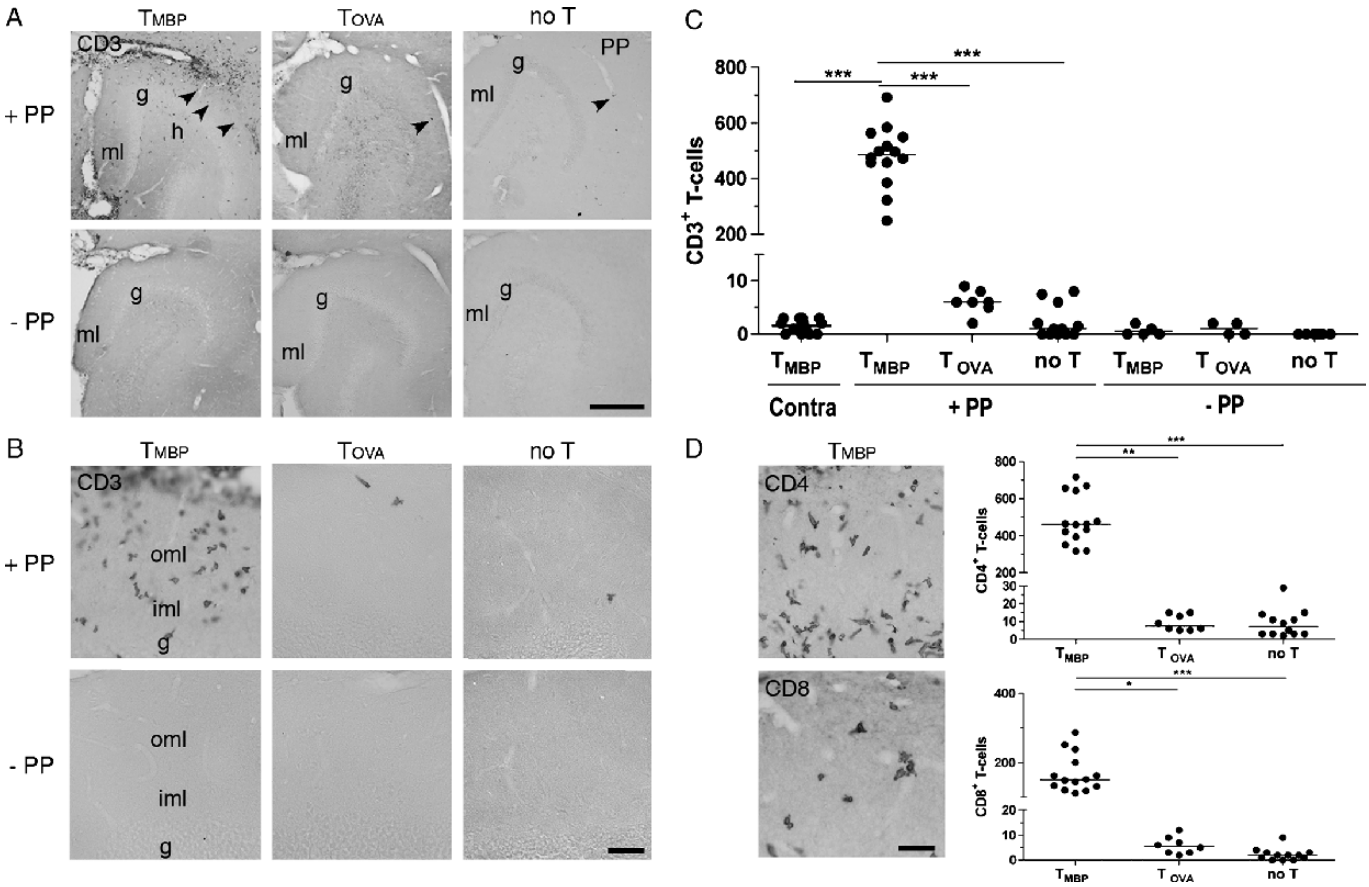

FIGURE 1. Targeting of myelin-reactive T cells to zones of axonal degeneration in the dentate gyrus. **(A, B)** Increased lesion-specific infiltration of CD3$^+$ T cells in perforant pathway (PP)-lesioned T_{MBP}-recipient mice 7 days after lesion. CD3 stain show greater infiltration of T cells in the molecular layer of PP-lesioned T_{MBP} animals (T_{MBP} +PP) (arrowheads) than in unlesioned T_{MBP} (T_{MBP} -PP), PP-lesioned T_{OVA} (T_{OVA} +PP), and naïve (no T +PP) mice. Virtually, no T cells were observed in unlesioned T cell-recipient and -naïve mice (**A**, **B**, bottom row). g indicates granule cell layer; h, hilus; ml, molecular layer; iml, inner molecular layer; oml, outer molecular layer. Bars: **(A)** 250 μm; **(B)** 20 μm. **(C)** Numbers of CD3$^+$ T cells in the molecular layer of mice 7 days after lesion. The lines indicate medians. ***$p < 0.001$. **(D)** Infiltrating T cells in PP-lesioned recipient and naïve animals are mainly CD4$^+$ cells with smaller numbers of CD8$^+$ cells. At 7 days after PP lesion in T_{MBP} animals, there are CD4$^+$ and CD8$^+$ cells in the molecular layer. Bar = 20 μm. Graphs show numbers of cells in PP-lesioned T_{MBP}, T_{OVA}, and naïve mice 7 days after lesion. The median for each group is marked with a line. The numbers of CD4$^+$ and CD8$^+$ cells in PP-lesioned T_{MBP} mice were significantly higher than in PP-lesioned T_{OVA} and naïve mice. *$p < 0.05$; **$p < 0.01$; ***$p < 0.001$.

gyrus compared with almost no infiltration in dentate gyrus of the unlesioned T_{MBP} mice (Fig. 1A, B), although these animals had developed clinical signs of EAE. $CD3^+$ T cells infiltrated the molecular layer of the dentate gyrus of lesioned by not nonlesioned mice (475 vs 5; $p < 0.001$) (Fig. 1C). The lesion specificity of the T-cell infiltration in the PP-lesioned T_{MBP} mice was additionally confirmed by observation of significantly larger numbers of $CD3^+$ T cells in the molecular layer of the deafferented ipsilateral dentate gyrus compared with the unlesioned contralateral dentate gyrus of the same mice (475 vs 2; $p < 0.001$) (Fig. 1C). Thus, T-cell infiltration was lesion specific in PP-lesioned T_{MBP} mice.

To determine whether the extent of T-cell infiltration depended on the antigen specificity of the injected T cells, we compared T-cell infiltration in the molecular layer in PP-lesioned and unlesioned T_{MBP}, T_{OVA}, and naïve mice. CD3+ T cells were particularly numerous in the oml of the dentate gyrus in the PP-lesioned T_{MBP} animals (Fig. 1A, B). $CD3^+$ T cells were also abundant in the meninges lining the deafferented dentate gyrus of T_{MBP} mice (Fig. 1A). A few $CD3^+$ T cells were also observed in the PP-lesioned T_{OVA} and naïve animals (Fig. 1A, B), whereas no T cells were observed in the molecular layer in unlesioned T_{MBP}, T_{OVA} mice, or naïve animals (Fig. 1A, B). Significantly more $CD3^+$ T cells infiltrated the molecular layer in PP-lesioned T_{MBP} mice compared with PP-lesioned T_{OVA} and PP-lesioned naïve mice (475 vs 7 and $p < 0.001$; 475 vs 1 and $p < 0.001$) (Fig. 1C). Cell counting also showed that the numbers of $CD3^+$ T cells were higher in the molecular layer of PP-lesioned naïve mice compared with naïve controls (1 vs 0; $p < 0.05$) (Fig. 1C).

To analyze the infiltration of T cells in lesioned animals in more detail, parallel sections from PP-lesioned and naïve mice were stained for CD4, a marker for MHC II-restricted T-helper/delayed-type hypersensitivity-type T cells (49) and CD8, a marker for MHC I-restricted cytotoxic T cells (50). As expected from analyses of T cells in EAE (7, 51), $CD4^+$ cells outnumbered $CD8^+$ cells (Fig. 1D); the combined numbers of $CD4^+$ and $CD8^+$ cells outnumbered the total number of $CD3^+$ cells. Significantly greater numbers of $CD4^+$ cells were observed in the molecular layer in PP-lesioned T_{MBP} mice than in PP-lesioned T_{OVA} and naïve mice (462 vs 7.5 and $p < 0.01$; 462 vs 7 and $p < 0.001$). This pattern was also observed with respect to numbers of $CD8^+$ T cells in PP-lesioned T_{MBP} mice compared with PP-lesioned T_{OVA} and naïve mice (151 vs 5.5, $p < 0.05$, and 151 vs 2, $p < 0.001$, respectively) (Fig. 1D). Because CD4 is inducible on activated microglia in rats (52), we also assessed CD4+ cell morphology; we observed no $CD4^+$ cells with ramified microglial morphology, that is, all cells had a rounded or amoeboid morphology (Fig. 1D).

T Cells Infiltrate the Neuropil in the Zone of Axonal Degeneration

T cells extravasate from the microvascular lumen into the perivascular space and from there cross the glia limitans to enter the neural parenchyma (53, 54). To distinguish between perivascular T-cell accumulation and infiltration of the parenchyma, we performed immunofluorescence double labeling for CD3 and laminin-1 (53, 55). $CD3^+$ T cells infiltrated the parenchyma of the ipsilateral dentate gyrus of PP-lesioned

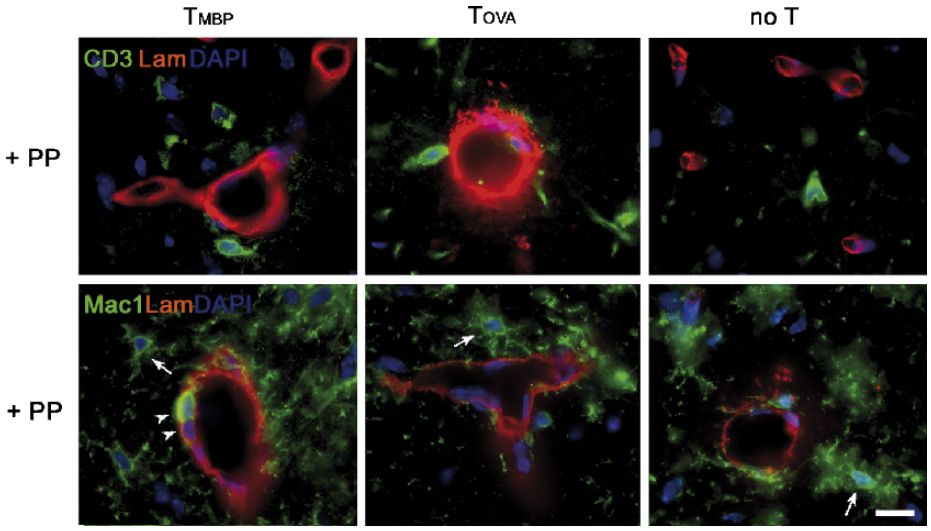

FIGURE 2. Perivascular and parenchymal infiltration of T cells and macrophages. **(Top row)** Double staining for CD3 (green) and laminin-1 (red), which stains the endothelial cells and astroglial basement membranes. There are more T cells in the neuropil of the perforant pathway (PP)-lesioned T_{MBP} than in the lesioned T_{OVA} and naïve mice. **(Bottom row)** Double staining for Mac-1 (green) and laminin-1 (red) shows accumulation of round $Mac\text{-}1^+$ cells in a PP-lesioned T_{MBP} mouse (arrowheads) and process-bearing cells in the parenchyma (arrows). In PP-lesioned T_{OVA} and naïve animals, only very limited perivascular accumulations were observed. Bar = 10 μm.

T_{MBP} mice, whereas only a few T cells entered the neuropil in PP-lesioned T_{OVA} and naïve mice (Fig. 2, arrowhead). This suggested that T cells within the neuropil in the PP-lesioned T_{MBP} mice could have direct effects on microglial cells in the zone of axonal lesion-induced myelin degeneration.

T Cells Enhance the Microglial Response to Axonal Degeneration in T_{MBP}-Recipient Mice

Reactive microgliosis was observed in the oml of the dentate gyrus in all PP-lesioned mice, whereas microglia in the unlesioned T cell-recipient and -naïve mice had the characteristics of resting microglia (16, 48) (Fig. 3A, B). In PP-lesioned T_{MBP} animals, the microglial response to axonal lesion was clearly greater than that in the PP-lesioned T_{OVA} and naïve animals. This was reflected in enhanced microglial density and/or upregulation of Mac-1 on the reactive microglia in the oml and the hilus of the dentate gyrus (Fig. 3A, B). Cell counts confirmed that there were significantly more Mac-1^+ microglia in PP-lesioned T_{MBP} mice than in PP-lesioned T_{OVA} (1,081 vs 501; $p < 0.01$) and naïve mice (1,081 vs 568; $p < 0.05$) (Fig. 3C). Most Mac-1^+ cells were process-bearing cells, that is, activated microglia (Fig. 3B, arrow), but there were a few round macrophage-like cells in T cell-recipient and -naïve PP-lesioned animals (Fig. 3B, arrowhead).

To determine the location of Mac-1^+ macrophage-like cells, parallel sections were double stained for Mac-1 and laminin-1. There were a few round Mac-1^+ cells in perivascular spaces of PP-lesioned T_{MBP} animals in the dentate gyrus oml, whereas there were process-bearing cells in the parenchyma (Fig. 2, arrows); there were also perivascular

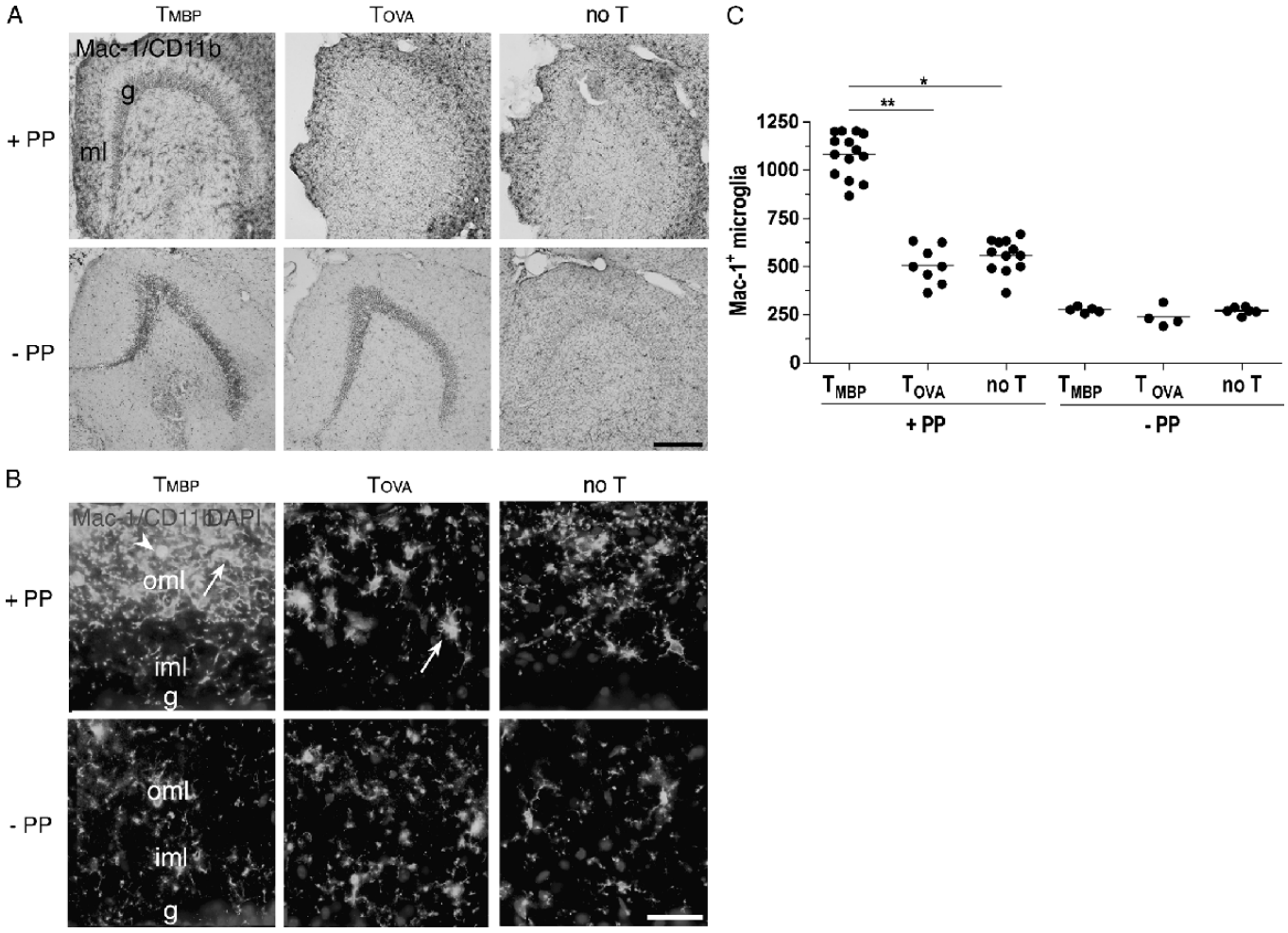

FIGURE 3. Infiltration with T_{MBP} cells enhances the microglial response to axonal lesion. **(A)** CD11b/Mac-1-stained sections show a greater axotomy-induced microglial reaction in the dentate gyrus of a perforant pathway (PP)-lesioned T_{MBP} mouse (T_{MBP} +PP) compared with PP-lesioned T_{OVA} (T_{OVA} +PP) and naïve (no T +PP) mice 7 days after lesion. Unlesioned (-PP) T cell-recipient and -naïve mice (bottom row) showed the characteristic morphology of resting microglia. **(B)** Fluorescent staining for CD11b/Mac-1 at high magnification. Most Mac-1^+ cells in lesioned mice seem to be process-bearing activated microglia (arrows) with only very few round macrophage-like cells (arrowhead). g indicates granule cell layer; h, hilus; iml, inner dentate molecular layer; ml, dentate molecular layer; oml, outer dentate molecular layer. Bars: **(A)** 200 μm; **(B)** 50 μm. **(C)** Numbers of Mac-1^+ microglia in the molecular layer of mice at 7 days after lesion. The lines indicate the medians. *$p < 0.05$; ***$p < 0.001$.

accumulations of Mac-1$^+$ macrophages in the meninges (not shown). Mac-1$^+$ macrophage-like cells were less frequent in the oml in PP-lesioned T_{OVA} and naïve animals than in the PP-lesioned T_{MBP} animals (Fig. 2).

Enhanced Clearance of Myelin Particles in T Cell–Recipient Mice

In unlesioned T cell–recipient mice and naïve control mice, there was a network of MBP$^+$ myelinated fibers in the oml, mainly in the medial perforant path zone and in the entrance area of the PP (Fig. 4A). As previously reported (37), transection of the PP resulted in a characteristic change in MBP immunostaining in the oml at day 7. Thus, in PP-lesioned animals, the MBP$^+$ myelinated fibers were replaced by particles of MBP$^+$ material (Fig. 4A), reflecting myelin disintegration and resulting in a score of 3 (Fig. 4B) (3 vs 0; $p < 0.001$). Myelin disintegration was greatest in the oml of PP-lesioned T_{MBP} mice (Fig. 4A). This was reflected by a reduction in the amount of MBP$^+$ particles in PP-lesioned T_{MBP} mice compared with PP-lesioned naïve mice (1 vs 3; $p < 0.01$) and to PP-lesioned T_{OVA} mice (1 vs 3; $p < 0.05$) (Fig. 4B). The PP-lesioned T_{OVA} mice showed a pattern of

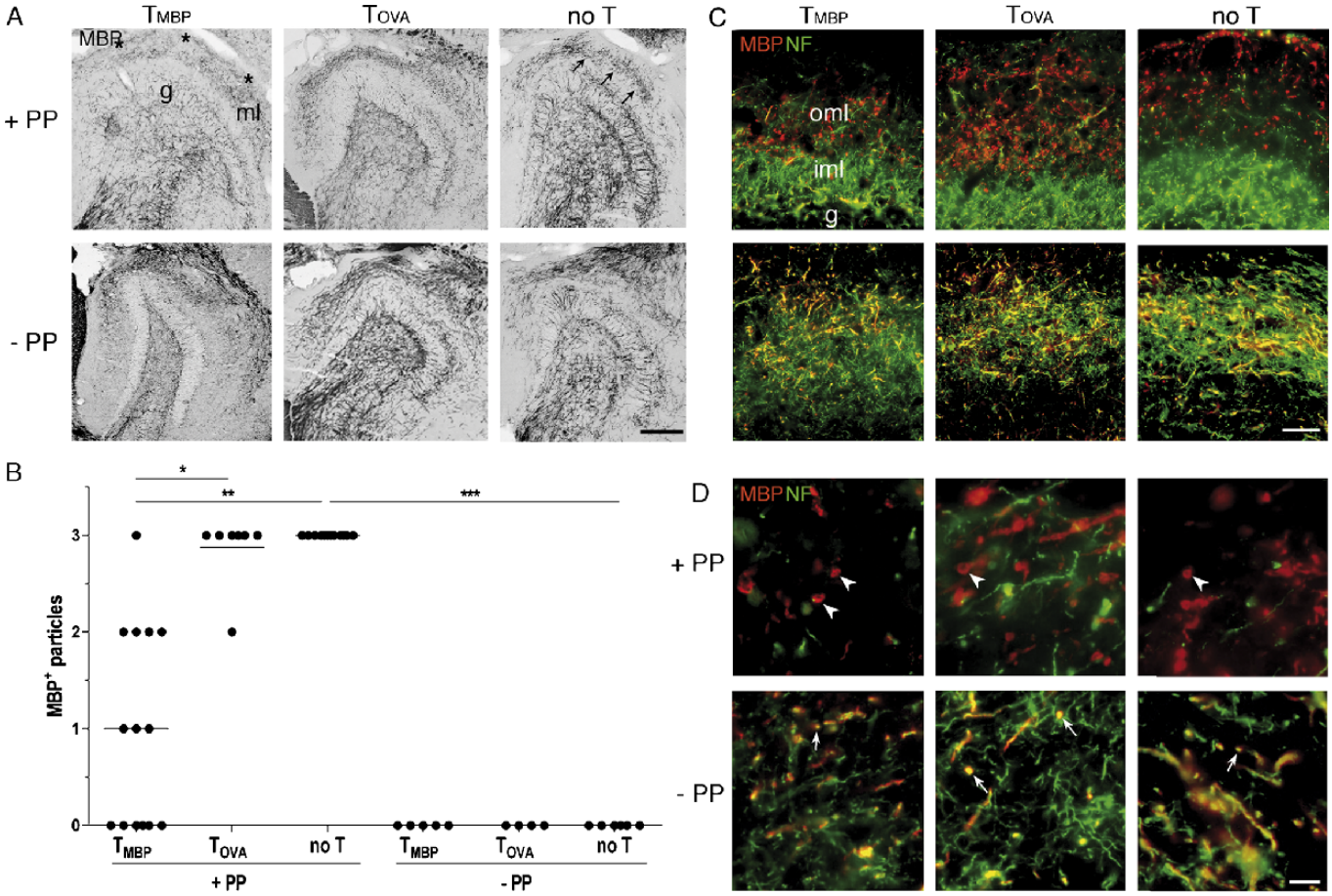

FIGURE 4. Enhanced clearing of myelin particles in perforant pathway (PP)-lesioned T_{MBP} mice. **(A)** Myelin basic protein-immunostained sections from PP-lesioned and unlesioned T_{MBP} (T_{MBP} +PP, T_{MBP} -PP) and T_{OVA} (T_{OVA} +PP, T_{OVA} -PP) mice and from a naïve mouse (no T +PP, no T -PP). Perforant pathway lesion results in disintegration of MBP$^+$ fibers and in the appearance of MBP$^+$ particles (arrows) compared with unlesioned naïve mice (no T-PP). Perforant pathway-lesioned T_{MBP} mice contained fewer MBP$^+$ particles (asterisks, T_{MBP} +PP) than PP-lesioned T_{OVA} (T_{OVA} +PP) and naïve mice (no T +PP). g indicates granule cell layer; iml, inner molecular layer; ml, molecular layer; oml, outer molecular layer. Bar = 100 μm. **(B)** PP-lesioned T_{MBP} mice contain fewer MBP$^+$ particles compared with PP-lesioned T_{OVA} and naïve mice 7 days after lesion. Unlesioned T cell-recipient and -naïve mice contained no MBP$^+$ particles. Lines indicate medians. *$p < 0.05$; **$p < 0.01$; ***$p < 0.001$. **(C)** Myelin debris is secondary to axonal degeneration, not autoimmune demyelination. Double immunofluorescence for MBP (red) and NF (green) provides a clear distinction between the MBP$^+$ particles in the oml in PP-lesioned T cell-recipient and -naïve mice (top row) and the double-labeled myelinated MBP$^+$NF$^+$ axons in unlesioned T cell-recipient and -naïve mice (bottom row). g indicates granule cell layer; iml, inner molecular layer; oml, outer molecular layer. Bar = 10 μm. **(D)** High magnification showing numerous cross-sectioned NF$^+$ fibers enwrapped in MBP$^+$ myelin (arrows) in unlesioned T cell-recipient and -naïve mice (bottom row). In contrast, in PP-lesioned T cell-recipient and -naïve mice (top row), the MBP$^+$ particles showed no colocalization with NF$^+$ axons. Several cross-sectioned MBP$^+$ structures appeared to have a hollow center, indicating degeneration of the enclosed axon (arrowheads). There are fewer MBP$^+$ particles in the T_{MBP} PP-lesioned mouse (T_{MBP} +PP). Bar = 2.5 μm.

myelin disintegration similar to that observed in PP-lesioned naïve mice (Fig. 4A, B). There was myelin disintegration in the unlesioned mice (Fig. 4A); all unlesioned mice were scored as having no particles (0 score) (Fig. 4B).

Axonal Degeneration Not Autoimmune Demyelination Leads to Accumulation of Myelin Debris

To verify that the MBP^+ particles observed in the PP-lesioned T cell-recipient mice and naïve animals were indeed myelin debris and not myelinated axons in cross-section, we performed double staining for MBP and NF. Sections were selected at the anatomical level that showed the highest amount of fibers in cross-section. In naïve animals, a broad band of NF^+ fibers colocalized with the MBP^+ fibers of the PP in the oml (Fig. 4C). At high magnification, numerous cross-sectioned fibers could be distinguished as NF^+ axons enwrapped by MBP^+ myelin (Fig. 4D). A similar pattern was observed in unlesioned T_{MBP} or T_{OVA} animals (Fig. 4D), thereby excluding autoimmune demyelination as the cause of myelin debris in our model. By contrast, there was almost complete absence of NF^+ axons and the MBP^+ myelinated fibers of the PP had been replaced by MBP^+ particles that showed no colocalization with NF in lesioned naïve animals (Fig. 4D). Perforant pathway-lesioned T_{OVA} animals had similar features, whereas there were significantly fewer MBP^+ particles in PP-lesioned T_{MBP} animals (Fig. 4C, D). High magnification confirmed that they showed no colocalization with NF^+ axons. Indeed, several of the cross-sectioned MBP^+ fibers appeared to have hollow centers, suggesting degeneration of the enclosed axon (Fig. 4D).

T-Cell Infiltration Enhances Microglial Phagocytosis of Myelin Debris

To confirm that microglial phagocytosis of myelin debris was stimulated as a consequence of infiltration by T_{MBP}, we performed double staining for MBP and Mac-1. Activated MBP-containing Mac-1^+ cells with microglial-like morphology were observed in all PP-lesioned T cell-recipient and -naïve mice; the intracellular location of MBP was validated by confocal analysis (Fig. 5C). Although PP-lesioned T_{MBP} animals showed numerous activated Mac-1^+ microglia containing MBP^+ particles (Fig. 5A), this was observed to a much lesser extent in PP-lesioned T_{OVA} and naïve animals; MBP^+ particles were absent in unlesioned recipient and naïve animals (Fig. 5A). There were significantly more

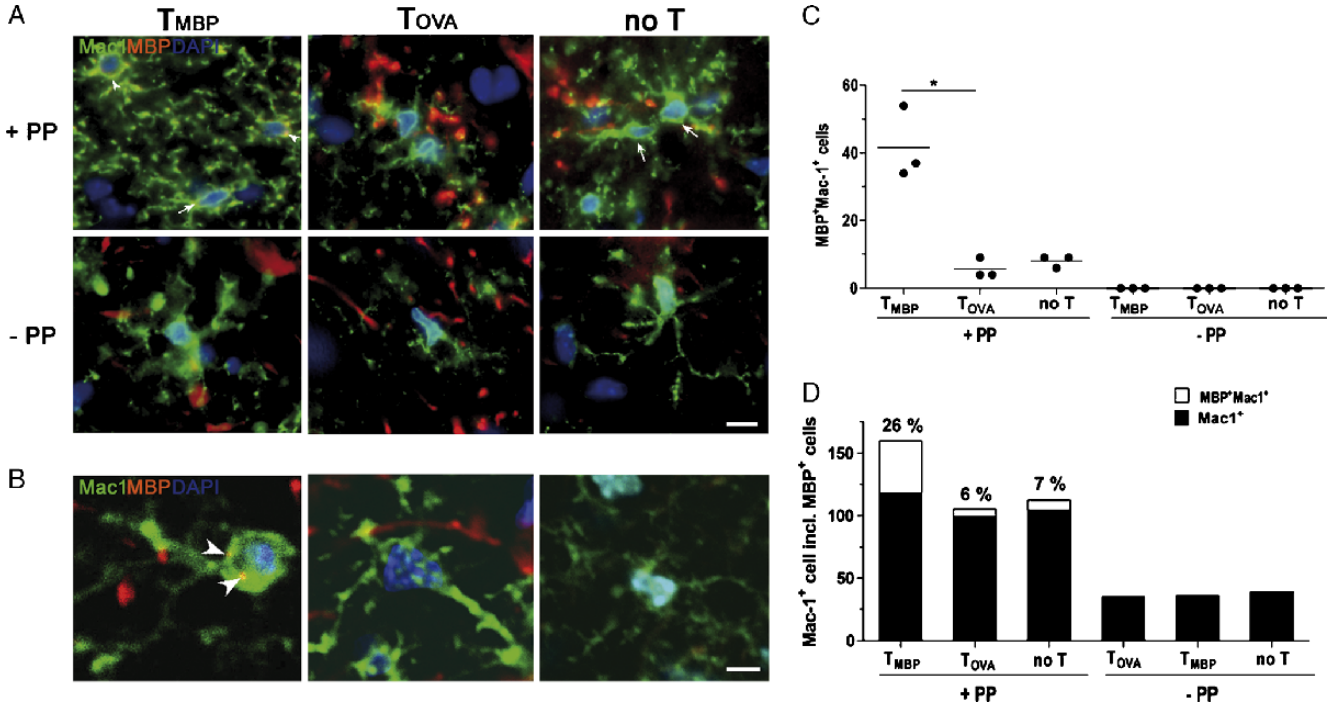

FIGURE 5. Microglia in perforant pathway (PP)-lesioned T_{MBP} mice show increased phagocytosis of myelin debris. **(A)** Immunofluorescence double staining for MBP (red) and Mac-1 (green) for visualization of myelin phagocytosis in the outer molecular layer (oml). Activated microglia (arrows) in PP-lesioned T cell-recipient and -naïve mice (top row) show colocalization with MBP (arrowheads), indicating phagocytosis; unlesioned T cell-recipient and -naïve mice (bottom row) showed resting microglia, intact myelin, and no colocalization. Bar = 10 μm. **(B)** Confocal laser scanning microscopy validates the intracellular localization of MBP^+ particles (arrowheads) in a Mac-1^+ cell of a PP-lesioned T_{MBP} mouse; activated microglia without MBP^+ myelin debris and resting microglia do not show intracellular localization. Bar = 5 μm. **(C)** Estimates of numbers and percentages of MBP^+ Mac-1^+ microglia in the oml of PP-lesioned and unlesioned T_{MBP}, T_{OVA}, and naïve mice (n = 3 per group). The numbers of MBP^+Mac-1^+ microglia were significantly higher in PP-lesioned T_{MBP} mice than in PP-lesioned T_{OVA} mice. *$p < 0.05$. **(D)** MBP^+Mac-1^+ microglia were more numerous in PP-lesioned T_{MBP} mice than in PP-lesioned T_{OVA} and naïve mice.

$MBP^+Mac\text{-}1^+$ cells in the oml of PP-lesioned T_{MBP} mice compared with the PP-lesioned T_{OVA} mice (42 vs 6; $p < 0.05$) (Fig. 5C). Compared with the total number of $Mac\text{-}1^+$ cells, 26% had incorporated MBP in the PP-lesioned T_{MBP} animals whereas only 6% and 7% had done so in the PP-lesioned T_{OVA} and naïve animals, respectively (Fig. 5D). Thus, the presence of T_{MBP} provided a strong stimulus for microglial phagocytosis of myelin debris in the zone of anterograde axonal degeneration in the deafferented dentate gyrus.

DISCUSSION

In this study, we show that axonal lesion of T cell-recipient mice results in a lesion-specific infiltration of myelin-reactive T cells into the zone of anterograde axonal and terminal degeneration within the dentate gyrus and that lesion-specific infiltration of myelin-reactive T cells enhances the microglial response and phagocytic clearance of MBP^+ myelin debris from the zone of axonal degeneration. These observations raise the possibility that axonal and terminal degeneration distal to sites of axonal transection could precipitate the development of new inflammatory lesions but also that certain aspects of T cell infiltration might prove beneficial to regenerative processes in the CNS.

For myelin-reactive T cells to exert an effect on the axonal lesion-reactive microglia and degenerating myelin, they must cross the vascular endothelium, the glia limitans, and the perivascular space between them (53, 54, 56). The first step of extravasation from the microvascular lumen into the perivascular space largely depends on interactions between integrins and selectins expressed on activated leukocytes and endothelial cells (57–59). For example, upregulation of intercellular adhesion molecule-1 on endothelial cells in the deafferented dentate gyrus has been previously observed (60). Another important factor for leukocyte infiltration is the intraparenchymal production of chemokines. The chemokine ligands (CCL) CCL2 and CCL5 have attracted particular attention due to their proposed role in attraction and retention of leukocytes to the CNS after inflammation and traumatic and ischemic injury (61, 62). Both chemokines are induced in the hippocampus after PP lesion (32, 46), and CCL2 influences the T-cell and macrophage infiltration into the PP-deafferented hippocampus (32).

In line with earlier studies on the PP-deafferented dentate gyrus in mice and rats (29–31, 37, 63), we observed only a minor lesion-induced recruitment of T cells into the deafferented dentate gyrus of naïve mice. A more pronounced effect was observed in previous studies in which T-cell infiltration was quantified using flow cytometry (32, 64). Several factors may contribute to this difference, one being the difference in brain region analyzed, which, in the flow cytometry study, encompassed the entire hippocampal formation. In addition, Bechmann et al (31) reported on axonal lesion-induced T-cell infiltration in areas with combined retrograde and anterograde degeneration in the hippocampal white matter (ie, alveus) in rats. Another reason could be that only intraparenchymal and not perivascular T cells were counted in the present study; T cells are frequently located in the perivascular spaces of perfused CNS.

Activated T cells enter the CNS and may accumulate at injury sites regardless of their antigen specificities (8, 26–28, 65, 66). Ovalbumin-specific T cells enter the CNS after adoptive transfer into SJL mice but do not cause demyelination or glial cell reaction (67). Because we observed no effect of T_{OVA} on the microglial response day 7 postlesion, we conclude that only the T_{MBP} had the ability to enhance the microglial response to axonal lesion and microglial clearance of myelin debris. This does not preclude the possibility that CNS-infiltrating T cells in the T_{OVA} or T_{MBP} mice were more numerous before day 7 postlesion, but T cells appeared to be retained to a greater extent in the lesioned T_{MBP} mice. In spinal cord injury, the infiltration of T_{MBP} and T_{OVA} is transient; T cells are present from 3 to 21 days postlesion (27). Alternatively, the larger numbers of T cells in the T_{MBP} mice might be due to an increased recruitment of endogenous T cells; this could not be assessed in the present study because the injected cells were not labeled. Indeed, at the onset of EAE, as many as 50% of CNS-infiltrating T cells have been determined to be naïve bystander T cells (40), and the numbers may be even larger in spinal cord injury (27). Although, we cannot exclude an effect of endogenous T cells in our study, observations by others suggests that the effect of endogenous T cells is marginal (27, 40, 68).

The CNS-infiltrating T_{MBP} cells were associated with significantly increased numbers of $Mac\text{-}1^+$ microglial cells in response to the axonal lesion compared with the CNS-infiltrating T_{OVA} cells. We and others have previously shown that the lesion-induced expansion of the microglial population can be attributed to proliferation and migration of resident microglia and, to a lesser extent, infiltration of bone marrow-derived microglia (46, 69–71). Because CNS-infiltrating T cells in T_{MBP} but not T_{OVA} mice (40) are known to produce proinflammatory cytokines such as interferon-γ (IFNγ), we speculate that cytokines produced by the T_{MBP} boosted the microglial response. Our group has shown that transgenic overexpression of IFNγ stimulates the axonal lesion-induced microglial reaction (72) whereas deficiency in tumor necrosis factor (TNF) or the two TNF receptors appeared to have no effect (38, 64). Alternatively, the T cells might have prevented or delayed the programmed microglial cell death that was shown to be prominent already 3 days after PP-lesion of the dentate gyrus (46).

In addition to microglia, it has been shown using flow cytometry that macrophages infiltrate the hippocampus in mice during the first 8 days after the lesion (32, 46, 64). These observations are in agreement with our present observation of a few $Mac\text{-}1^+$ cells of a round morphology in PP-lesioned mice and raise the possibility that blood-borne macrophages might contribute to the clearance of myelin debris. Although this is possible, we observed that most $Mac\text{-}1^+$ cells, including all the $Mac\text{-}1^+$ cells that had phagocytosed MBP^+ debris, had typical reactive process-bearing microglial morphology rather than a round macrophage-like morphology. This is in agreement with a more predominant role of microglia than blood-borne macrophages in myelin phagocytosis in rats with EAE (73) and with more recent observations that depletion of blood-borne macrophages had

only modest effects on microglial expansion and no effect on infiltrating T cells or TNF mRNA expression in PP-lesioned naïve mice (74).

The appearance of MBP^+ particles correlates with the degree of axonal degeneration after PP lesion (36, 37) but could also be explained by autoimmune demyelination, as observed in EAE (7). Because only a few MBP^+ particles were observed in unlesioned animals that received T_{MBP} or T_{OVA}, we feel confident that the deposition of MBP^+ particles was initiated by PP lesion-induced Wallerian degeneration. Clearing of degenerating axons and myelin debris after Wallerian degeneration is usually considered slow and incomplete in CNS (20). This has also been shown for the PP lesion, where MBP^+ particles remain in the deafferented oml for weeks until removed by phagocytic cells (17, 37). The observation of reduced amounts of MBP^+ particles in PP-lesioned T_{MBP} mice compared with PP-lesioned T_{OVA} and naïve mice provides evidence that the CNS-infiltrating myelin-reactive T cells enhanced microglial clearance of myelin debris. This was additionally confirmed by the observation of increased numbers of Mac-1^+ microglia that contained intracellular MBP^+ material in PP-lesioned T_{MBP} mice compared with PP-lesioned T_{OVA} and naïve mice. The fact that MBP-containing Mac-1^+ microglia were also observed in PP-lesioned T_{OVA} and naïve mice is in line with observations of microglia being the principal phagocytosing cells after PP lesion in naïve animals (17).

It is becoming increasingly clear that T cells, particularly $CD4^+$ T cells, can influence the functional properties of microglia and other types of antigen-presenting cells (15). Activated microglia show increased phagocytosis of myelin in the presence of T cells, possibly through IL-2 secretion (75). Small amounts of $CD4^+$ Th1 cell-produced IFNγ stimulate glutamate uptake by microglia, which is neuroprotective (76). The observed effects might also be due to $CD4^+$ Th2 cells producing IL-4 because activated microglia cultivated in the presence of IL-4 downregulate the production of TNF and upregulate insulin-like growth factor-1 (77); the latter is neuroprotective and a stimulant of oligodendrogenesis (78). Similarly, Beers et al (79) showed that $CD4^+$ T cells affect IL-4 and TNF synthesis in vivo in a chronic model for neurodegeneration. In combination with our previous observation of IFNγ-mediated enhancement of microglial Mac-1/CD11b expression in PP deafferented dentate gyrus, this raises the possibility that IFNγ-producing $CD4^+$ Th1 cells stimulated microglial phagocytosis of MBP^+ debris after axonal lesion in the present study. This would be in agreement with observations of a role for Mac-1/CD11b in complement-mediated phagocytosis of degenerating synapses (80) and degenerated myelin (81, 82). Interestingly, however, Gimsa et al (83) showed that, although MBP-specific T cells induced microglia to attack myelinated axons in entorhinal-hippocampal slice cultures, IFNγ alone had no effect.

In conclusion, our results show that myelin-reactive T cells enhance microglial response to axonal lesion and enhance microglial phagocytic capacity. Understanding the mechanisms involved could prove beneficial in promoting regenerative processes after CNS axon and myelin injury.

ACKNOWLEDGMENTS

Confocal microscopy was performed with the assistance of Per Sveningsen. Statistical advice from professor of medical statistics Werner Vach and technical assistance by Lene Jørgensen and Sussanne Petersen are also greatly acknowledged.

REFERENCES

1. Raine CS. The neuropathology of multiple sclerosis. In: Raine CS, McFarland HF, Tourtellotte WW, eds. *Multiple Sclerosis: Clinical and Pathogenic Basis*. London: Chapman & Hall, 1997:151–71
2. Weiner HL. Multiple sclerosis is an inflammatory T cell–mediated autoimmune disease. Arch Neurol 2004;61:1613–15
3. Lucchinetti C, Brück W, Parisi J, et al. Heterogeneity of multiple sclerosis lesions: Implications for the pathogenesis of demyelination. Annals Neurol 2000;47:707–17
4. Zhang J, Markovic–Plese S, Lacet B, et al. Increased frequency of interleukin 2–responsive T cells specific for myelin basic protein and proteolipid protein in peripheral blood and cerebrospinal fluid of patients with multiple sclerosis. J Exp Med 1994;179:973–84
5. Petry KG, Boullerne AI, Pousset F, et al. Experimental allergic encephalomyelitis animal models for analyzing features of multiple sclerosis. Pathol- Biologie 2000;48:47–53
6. Gold R, Linington C, Lassmann H. Understanding pathogenesis and therapy of multiple sclerosis via animal models: 70 years of merits and culprits in experimental autoimmune encephalomyelitis research. Brain 2006;129:1953–71
7. Zamvil S, Nelson P, Trotter J, et al. T cell clones specific for myelin basic protein induce chronic relapsing paralysis and demyelination. Nature 1985;317:355–58
8. Moalem G, Leibowitz–Amit R, Yoles E, et al. Autoimmune T cells protect neurons from secondary degeneration after central nervous system axotomy. Nature Med 1999;5:49–55
9. Hauben E, Butovsky O, Nevo U, et al. Passive or active immunization with myelin basic protein promotes recovery from spinal cord contusion. J Neurosci 2000;20:6421–30
10. Frenkel D, Huang Z, Maron R, et al. Neuroprotection by IL-10–producing MOG CD4+ T cells following ischemic stroke. J Neurol Sci 2005;233:125–32
11. Besser M, Wank R. Cutting edge: Clonally restricted production of the neurotrophins brain-derived neurotrophic factor and neurotrophin-3 mRNA by human immune cells and Th1/Th2-polarized expression of their receptors. J Immunol 1999;162:6303–6
12. Stadelmann C, Kerschensteiner M, Misgeld T, et al. BDNF and gp145trkB in multiple sclerosis brain lesions: Neuroprotective interactions between immune and neuronal cells? Brain 2002;125:75–85
13. Cohen IR, Schwartz M. Autoimmune maintenance and neuroprotection of the central nervous system. J Neuroimmunol 1999;100:111–14
14. Napoli I, Neumann H. Microglial clearance function in health and disease. Neuroscience 2009;158:1030–38
15. Schwartz M, Butovsky O, Brück W, et al. Microglial phenotype: Is the commitment reversible? Trends Neurosci 2006;29:68–74
16. Streit WJ, Walter SA, Pennell NA. Reactive microgliosis. Prog Neurobiol 1999;57:563–81
17. Bechmann I, Nitsch R. Astrocytes and microglial cells incorporate degenerating fibers following entorhinal lesion: A light, confocal, and electron microscopical study using a phagocytosis-dependent labeling technique. Glia 1997;20:145–54
18. George R, Griffin JW. Delayed macrophage responses and myelin clearance during Wallerian degeneration in the central nervous system: The dorsal radiculotomy model. Exp Neurol 1994;129:225–36
19. Bignami A, Ralston HJ 3rd. The cellular reaction to Wallerian degeneration in the central nervous system of the cat. Brain Res 1969; 13:444–61
20. Vargas ME, Barres BA. Why is Wallerian degeneration in the CNS so slow? Ann Rev Neurosci 2007;30:153–79
21. Kotter MR, Li WW, Zhao C, et al. Myelin impairs CNS remyelination by inhibiting oligodendrocyte precursor cell differentiation. J Neurosci 2006;26:328–32

22. Schwab ME. Myelin-associated inhibitors of neurite growth and regeneration in the CNS. Trends Neurosci 1990;13:452–56
23. Foote AK, Blakemore WF. Inflammation stimulates remyelination in areas of chronic demyelination. Brain 2005;128:528–39
24. Neumann H, Kotter MR, Franklin RJ. Debris clearance by microglia: An essential link between degeneration and regeneration. Brain 2009;132: 288–95
25. Shaked I, Porat Z, Gersner R, et al. Early activation of microglia as antigen-presenting cells correlates with T cell–mediated protection and repair of the injured central nervous system. Journal Neuroimmunol 2004;146:84–93
26. Molleston MC, Thomas ML, Hickey WF. Novel major histocompatibility complex expression by microglia and site-specific experimental allergic encephalomyelitis lesions in the rat central nervous system after optic nerve transection. Adv Neurol 1993;59:337–48
27. Hirschberg DL, Moalem G, He J, et al. Accumulation of passively transferred primed T cells independently of their antigen specificity following central nervous system trauma. J Neuroimmunol 1998;89:88–96
28. Maehlen J, Olsson T, Zachau A, et al. Local enhancement of major histocompatibility complex (MHC) class I and II expression and cell infiltration in experimental allergic encephalomyelitis around axotomized motor neurons. J Neuroimmunol 1989;23:125–32
29. Fagan AM, Gage FH. Mechanisms of sprouting in the adult central nervous system: Cellular responses in areas of terminal degeneration and reinnervation in the rat hippocampus. Neuroscience 1994;58:705–25
30. Jensen MB, Finsen B, Zimmer J. Morphological and immunophenotypic microglial changes in the denervated fascia dentata of adult rats: Correlation with blood–brain barrier damage and astroglial reactions. Exp Neurol 1997;143:103–16
31. Bechmann I, Peter S, Beyer M, et al. Presence of B7–2 (CD86) and lack of B7–1 (CD(80) on myelin phagocytosing MHC-II–positive rat microglia is associated with nondestructive immunity in vivo. FASEB J 2001; 15:1086–88
32. Babcock AA, Kuziel WA, Rivest S, et al. Chemokine expression by glial cells directs leukocytes to sites of axonal injury in the CNS. J Neurosci 2003;23:7922–30
33. Berger T, Frotscher M. Distribution and morphological characteristics of oligodendrocytes in the rat hippocampus in situ and in vitro: An immunocytochemical study with the monoclonal Rip antibody. J Neurocytol 1994;23:61–74
34. Finsen B, Jensen MB, Lomholt ND, et al. Axotomy-induced glial reactions in normal and cytokine transgenic mice. Adv Exp Med Biol 1999;468:157–71
35. Matthews DA, Cotman C, Lynch G. An electron microscopic study of lesion-induced synaptogenesis in the dentate gyrus of the adult rat. I. Magnitude and time course of degeneration. Brain Res 1976; 115:1–21
36. Jensen MB, Gonzalez B, Castellano B, et al. Microglial and astroglial reactions to anterograde axonal degeneration: A histochemical and immunocytochemical study of the adult rat fascia dentata after entorhinal perforant path lesions. Exp Brain Res Experimentelle Hirnforschung 1994;98:245–60
37. Jensen MB, Hegelund IV, Poulsen FR, et al. Microglial reactivity correlates to the density and the myelination of the anterogradely degenerating axons and terminals following perforant path denervation of the mouse fascia dentata. Neuroscience 1999;93:507–18
38. Fenger C, Drojdahl N, Wirenfeldt M, et al. Tumor necrosis factor and its p55 and p75 receptors are not required for axonal lesion–induced microgliosis in mouse fascia dentata. Glia 2006;54:591–605
39. Meier S, Brauer AU, Heimrich B, et al. Myelination in the hippocampus during development and following lesion. Cell Mol Life Sci 2004;61: 1082–94
40. Krakowski ML, Owens T. Naïve T lymphocytes traffic to inflamed central nervous system, but require antigen recognition for activation. European J Immunol 2000;30:1002–9
41. Zeine R, Owens T. Direct demonstration of the infiltration of murine central nervous system by Pgp-1/CD44high CD45RB(low) CD4+ T cells that induce experimental allergic encephalomyelitis. J Neuroimmunol 1992;40:57–69
42. Nielsen HH, Ladeby R, Drojdahl N, et al. Axonal degeneration stimulates the formation of NG2+ cells and oligodendrocytes in the mouse. Glia 2006;54:105–15
43. Flügel A, Berkowicz T, Ritter T, et al. Migratory activity and functional changes of green fluorescent effector cells before and during experimental autoimmune encephalomyelitis. Immunity 2001;14:547–60
44. Perry VH, Hume DA, Gordon S. Immunohistochemical localization of macrophages and microglia in the adult and developing mouse brain. Neuroscience 1985;15:313–26
45. West MJ, Ostergaard K, Andreassen OA, et al. Estimation of the number of somatostatin neurons in the striatum: An in situ hybridization study using the optical fractionator method. J Comp Neurol 1996;370:11–22
46. Wirenfeldt M, Dissing–Olesen L, Anne Babcock A, et al. Population control of resident and immigrant microglia by mitosis and apoptosis. Am J Pathol 2007;171:617–31
47. Dissing–Olesen L, Ladeby R, Nielsen HH, et al. Axonal lesion–induced microglial proliferation and microglial cluster formation in the mouse. Neuroscience 2007;149:112–22
48. Ladeby R, Wirenfeldt M, Garcia–Ovejero D, et al. Microglial cell population dynamics in the injured adult central nervous system. Brain Res 2005;48:196–206
49. Miceli MC, Parnes JR. Role of CD4 and CD8 in T cell activation and differentiation. Advances Immunol 1993;53:59–122
50. Gao GF, Jakobsen BK. Molecular interactions of coreceptor CD8 and MHC class I: The molecular basis for functional coordination with the T cell receptor. Immunol Today 2000;21:630–36
51. Owens T, Sriram S. The immunology of multiple sclerosis and its animal model, experimental allergic encephalomyelitis. Neurol Clin NA 1995; 13:51–73
52. Perry VH, Gordon S. Modulation of CD4 antigen on macrophages and microglia in rat brain. J Exp Med 1987;166:1138–43
53. Toft–Hansen H, Buist R, Sun XJ, et al. Metalloproteinases control brain inflammation induced by pertussis toxin in mice overexpressing the chemokine CCL2 in the central nervous system. J Immunol 2006;177: 7242–49
54. Owens T, Bechmann I, Engelhardt B. Perivascular spaces and the two steps to neuroinflammation. J Neuropathol Exp Neurol 2008;67:1113–21
55. Sixt M, Engelhardt B, Pausch F, et al. Endothelial cell laminin isoforms, laminins 8 and 10, play decisive roles in T cell recruitment across the blood–brain barrier in experimental autoimmune encephalomyelitis. J Cell Biol 2001:153;933–46
56. Bechmann I, Galea I, Perry VH. What is the blood–brain barrier (not)? Trends Immunol 2007;28:5–11
57. McCandless EE, Piccio L, Woerner BM, et al. Pathological expression of CXCL12 at the blood–brain barrier correlates with severity of multiple sclerosis. Am J Pathol 2008;172:799–808
58. Laschinger M, Engelhardt B. Interaction of alpha4-integrin with VCAM-1 is involved in adhesion of encephalitogenic T cell blasts to brain endothelium but not in their transendothelial migration in vitro. J Neuroimmunol 2000;102:32–43
59. Piccio L, Rossi B, Scarpini E, et al. Molecular mechanisms involved in lymphocyte recruitment in inflamed brain microvessels: Critical roles for P-selectin glycoprotein ligand–1 and heterotrimeric G(i)–linked receptors. J Immunol 2002;168:1940–49
60. Wirenfeldt M, Dissing–Olesen L, Babcock AA, et al. Microglial cell population expansion following acute neuronal injury. In: Malva J, Rego AC, Cunha R, Oliveira CR, eds. *Interaction Between Neurons and Glia in Aging and Disease*: Springer, 2007
61. Ransohoff RM, Tani M. Do chemokines mediate leukocyte recruitment in post-traumatic CNS inflammation? Trends Neurosci 1998;21:154–59
62. Ransohoff RM. Mechanisms of inflammation in MS tissue: Adhesion molecules and chemokines. J Neuroimmunol 1999;98:57–68
63. Babcock AA, Toft–Hansen H, Owens T. Signaling through MyD88 regulates leukocyte recruitment after brain injury. J Immunol 2008;181: 6481–90
64. Babcock AA, Wirenfeldt M, Holm T, et al. Toll-like receptor 2 signaling in response to brain injury: An innate bridge to neuroinflammation. J Neurosci 2006;26:12826–37
65. Hickey WF, Hsu BL, Kimura H. T-lymphocyte entry into the central nervous system. Journal Neurosci Res 1991;28:254–60
66. Ling C, Sandor M, Suresh M, et al. Traumatic injury and the presence of antigen differentially contribute to T cell recruitment in the CNS. J Neurosci 2006;26:731–41
67. Smorodchenko A, Wuerfel J, Pohl EE, et al. CNS-irrelevant T cells enter the brain, cause blood–brain barrier disruption but no glial pathology. Eur J Neurosci 2007;26:1387–98

68. Lu HZ, Xu L, Zou J, et al. Effects of autoimmunity on recovery of function in adult rats following spinal cord injury. Brain Behav Immunity 2008 [Epub ahead of print].
69. Ladeby R, Wirenfeldt M, Dalmau I, et al. Proliferating resident microglia express the stem cell antigen CD34 in response to acute neural injury. Glia 2005;50:121–31
70. Priller J, Flügel A, Wehner T, et al. Targeting gene-modified hematopoietic cells to the central nervous system: Use of green fluorescent protein uncovers microglial engraftment. Nat Med 2001;7:1356–61
71. Rappert A, Bechmann I, Pivneva T, et al. CXCR3-dependent microglial recruitment is essential for dendrite loss after brain lesion. J Neurosci 2004;24:8500–9
72. Jensen MB, Hegelund IV, Lomholt ND, et al. IFNgamma enhances microglial reactions to hippocampal axonal degeneration. J Neurosci 2000;20:3612–21
73. Rinner WA, Bauer J, Schmidts M, et al. Resident microglia and hematogenous macrophages as phagocytes in adoptively transferred experimental autoimmune encephalomyelitis: An investigation using rat radiation bone marrow chimeras. Glia 1995;14:257–66
74. Fux M, van Rooijen N, Owens T. Macrophage-independent T cell infiltration to the site of injury-induced brain inflammation. J Neuroimmunol 2008;203:64–72
75. Ghasemlou N, Jeong SY, Lacroix S, et al. T cells contribute to lysophosphatidylcholine-induced macrophage activation and demyelination in the CNS. Glia 2007;55:294–302
76. Shaked I, Tchoresh D, Gersner R, et al. Protective autoimmunity: interferon-gamma enables microglia to remove glutamate without evoking inflammatory mediators. J Neurochem 2005;92:997–1009
77. Butovsky O, Talpalar AE, Ben–Yaakov K, et al. Activation of microglia by aggregated beta-amyloid or lipopolysaccharide impairs MHC-II expression and renders them cytotoxic whereas IFN-gamma and IL-4 render them protective. Molec Cell Neurosci 2005;29:381–93
78. Butovsky O, Landa G, Kunis G, et al. Induction and blockage of oligodendrogenesis by differently activated microglia in an animal model of multiple sclerosis. J Clin Invest 2006;116:905–15
79. Beers DR, Henkel JS, Zhao W, et al. CD4+ T cells support glial neuroprotection, slow disease progression, and modify glial morphology in an animal model of inherited ALS. Proc Nat Acad Sci USA 2008;105:15558–63
80. Stevens B, Allen NJ, Vazquez LE, et al. The classical complement cascade mediates CNS synapse elimination. Cell 2007;131:1164–78
81. Bullard DC, Hu X, Schoeb TR, et al. Critical requirement of CD11b (Mac-1) on T cells and accessory cells for development of experimental autoimmune encephalomyelitis. J Immunol 2005;175:6327–33
82. Stapulionis R, Pinto Oliveira CL, Gjelstrup MC, et al. Structural insight into the function of myelin basic protein as a ligand for integrin αM(2. J Immunol 2008;180:3946–56
83. Gimsa U, Peter SV, Lehmann K, et al. Axonal damage induced by invading T cells in organotypic central nervous system tissue in vitro: Involvement of microglial cells. Brain Pathol 2000;10:365–77